

## CREEP DAMAGE AND CRACK GROWTH IN STEEL WELDS

Bilal DOGAN, GKSS Research Centre, Max-Planck-Str., D-21502 Geesthacht, Germany

The operational experience in high temperature plants indicates that in the majority of cases where creep crack initiation and growth occurs, defects predominate in the vicinity of weldments. The state of the art in time dependent fracture analysis is that the concepts used for homogeneous bodies are commonly applied to creep crack growth in weldments. The crack growth rate is correlated with  $C^*(t)$  in the extensive creep regime according to ASTM standard E1457. However, specific issues pertinent to welds such as deformation and crack growth behaviour due to the variations in microstructure through weld cross-section and brittle HAZ call for a systematic study, as addressed in the present work. This paper reports on the creep deformation behaviour and analysis of crack growth data obtained on high strength martensitic steel Grade P91 similar welds at 600°C. The weldments were produced in pipe butt weld geometry. The tests were carried out on cross-weld compact tension, CT, type specimens for tests durations of 300 to 4000 hrs that produced crack growth data in small-scale creep to extensive creep ranges for welds and HAZs. The emphasis is placed on the test procedure and the crack tip parameters in correlating the creep crack growth in weldments that will lead to provision of guidelines for acceptable methodologies for assessment and analysis of laboratory creep crack growth test data of weldments.

**Key Words:** Creep crack growth,  $C^*(t)$ -integral, Data analysis, Defect assessment, Buttwelding, Similar welds, HAZ, P91 steel weld.

### 1. INTRODUCTION

The failures in industrial components in power generating and petrochemical plants operating under high temperature creep conditions occur more frequently in welds and associated heat affected zones (HAZ). Due to the composite structure of weldments consisting of a base metal (BM) and a weld metal (WM), different mechanical and creep properties need to be considered. Furthermore, the interface region between BM and WM shows a considerable microstructure/property gradient that extends from the fusion region of the weld metal through the HAZ of the BM.

Defect assessment of weldments requires determination of the properties characterizing the resistance of the constituent microstructures to crack growth. In high temperature plant components exercising primary (applied stress) and/or secondary (residual stress) loading the damage is dominated by creep mechanisms [1]. The weldments exercise complex distribution of stress and temperature, however, the creep properties from uniaxial testing under isothermal conditions are used for crack growth and defect assessment of components. Hence, the prerequisite for a reliable defect assessment is that the laboratory data are meaningful [2]. Therefore, the testing and analysis techniques for welds require consideration of homogeneous microstructure, limited ductility and smaller deformation zone size associated with defect incubation and propagation. In the case of HAZ the change of microstructure in the range of fine to coarse grain size requires notch positioning inside this region that affect the crack growth behaviour of HAZ material. At present guidelines are not available for the consideration and treatment of these aspects. Current approaches for predicting creep crack growth in weldments are based entirely on concepts developed for homogeneous materials [3]. The crack growth rate is correlated with  $C^*(t)$  in the extensive creep regime according to ASTM E1457 [4], the only available standard for creep crack growth testing of metallic materials, and with  $C_t$  parameter [5] in the small scale creep to the extensive creep regimes. However, recent experimental data [6,7] and analytical evidence [8,9] has shown that  $C^*(t)$  is not suitable for characterizing creep crack growth behaviour in materials with low ductility in which the crack tip can advance at a rate comparable to the creep zone expansion rate. This directs attention to the crack tip parameters that correlate data in both creep ductile and creep brittle

materials, such as  $K_t$ ,  $C_t$ , and Crack Tip Opening Displacement (CTOD) rate measured at crack tip that may potentially include transition tails in early crack growth correlations [10].

Linear elastic and elastic-plastic analyses of bimaterial interface cracks show that the crack tip fields and shapes and sizes of plastic zones are different for homogeneous bodies and bimaterials. Also, even though the nominal loading is Mode I, the interface experiences a combined Mode I and Mode II loading. Hence, a rigorous treatment of elastic-plastic fracture and creep crack growth in welded structures is beyond the current capability of fracture mechanics. Consequently, somewhat ad hoc correlation procedures are presently available, although without rigorous justification [3]. However, as the experimental work [4,6,7] clearly demonstrated the promise of such approaches, and considerable progress has been made in the determination, analytical representation and application of creep crack growth (CCG) property data during the past three decades [11-15].

The present paper reports on the systematic work initiated on martensitic P91 steel weldments at 600°C to address the technical and industrial need to provide guidelines for testing compact tension (CT) specimens and data analysis of welds and HAZs. This consequently will increase the reliability of laboratory data produced and the ensuing structural integrity predictions. The programme will serve harmonization and development of testing and data analysis procedures for characterizing the creep crack growth (CCG) behaviour of weldments using CT specimens.

### 2. MATERIALS AND METHODS

The experimental material, ASTM P91 (Mod. 9Cr1Mo) steel, is a newly developed high strength, high ductility martensitic steel with possible applications in pressure parts in conventional and nuclear power plant, and petrochemical reactor vessels and pipework.

Welded pipes were produced by circumferential butt welding using shielded metal arc welding (SMAW) process. Metallographic sample sections showed a good quality weld with refined microstructure and little evidence of coarse grains of the weld fusion line that is sometimes observed in industrial welds.

The material for simulated HAZ, used for mechanical and creep property determination, was produced by thermal cycling in a Gleeble weld simulator machine. The simulated material had the microstructure and hardness of real weld HAZ's. An analytical method [16,17] was used in HAZ simulation for the calculation of the time between 800°C and 500°C during welding. This time is considered critical for the resulting microstructure and hardness of the material.

The test materials were taken from the welded pipes of 295mm outer diameter and 55mm wall-thickness. The pipes were PWHT'ed at 760°C prior to sectioning of blanks for machining of the specimens.

### 2.1 Specimens

Standard tensile and creep test specimens were machined from both the welded material and simulated HAZ material. Crack growth test specimens were machined from the weldments with the notches introduced by electrical discharge method (EDM) in WM and HAZ, both in the centre of HAZ and TypeIV region. The CCG specimens of CT25 type (W=25mm, B=12.5mm) were side grooved 20% after EDM notching to  $a_0/W=0.5$ , with notch tip radius of 0.05mm for a sharp starter crack.

### 2.2 Testing

Mechanical and uniaxial creep rupture tests were carried out at 600°C. CCG tests were done at the same temperature as in mechanical and creep rupture tests using direct current potential drop (DCPD) method for crack size monitoring during testing. Deflection on the load line was measured directly on the specimen surface using laser scanner system [19]. The applied constant loads were calculated from predetermined initial K levels for the given test durations. Target test durations were 500h, 2000h and 4000h, with the main concern of acquisition of valid creep crack growth data.

### 2.3 Data Analysis

The experimental crack growth data were analysed following the guidelines below.

**2.3.1 Determination of crack length:** The crack length was determined from the direct current potential drop reading (DCPD) on the specimens with lead positions as described in ASTM E1457 Annex A1.1 [4]. If the thermal voltage ( $V_{th}$ ) was considerable, the values of  $V_{th}$  were subtracted from the indicated values of  $V$  and  $V_0$  before substituting them in Johnson's formula [4].

The predicted crack extension,  $\Delta a_{pf}$ , was calculated by subtracting the initial crack length,  $a_0$ , from the predicted value of the final crack length,  $a_{pf}$ . The initial crack length,  $a_0$ , and the final crack size,  $a_f$ , were calculated from the measurements made on the fracture surface at nine equally spaced points centered on the specimen mid-thickness line.

**2.3.2 Validation of Test:** The data were valid for further processing when

$$0.85 \leq (\Delta a_{pf} / (a_f - a_0)) \leq 1.15 \quad (1)$$

If the above was not satisfied the difference between the predicted and calculated crack growth was noted and the data was further processed.

The fact that due to crack front irregularities and crack tunneling the crack length values determined on fracture surfaces may vary from the calculated ones using DCPD. It, mainly, depends on the way the crack length measurement is made on the fracture surface. Therefore, the measurements were made on the fracture surface along the crack front, ignoring the unbroken ligaments. The individual measurements on fracture surface also vary due to crack front irregularities. The difference between the determined and calculated values was reported.

**2.3.3 Determination of crack growth and load-line displacement rate:** The crack length, load-line deflection and time data were processed for determining crack growth rate and the load-line displacement rate using the secant method [4]. The time and load line displacements were set to zero at initial crack size  $a_0$ . Subsequent data points were chosen consisting of crack length and the corresponding load-line displacement and time such that crack extension between successive data points is 0.005W. If the crack growth was small, smaller  $\Delta a$  values were taken such that minimum nine successive rate data points will be determined for the total crack growth range.

**2.3.4 Determination of  $C^*(t)$ -integral:** From the recorded data the magnitude of the  $C^*(t)$ -integral was determined along with K at each point following the test standard ASTM E1457 [4].

**2.3.5 Validity Criteria:** The following validity criteria were satisfied for the data to be considered valid. However, due to difficulties in testing and crack growth behaviour of weldments all the data were reported together with the data satisfying the validity criteria.

- a) Only the data for which  $t \geq t_T$  are taken for valid, where  $t$  is the test time,  $t_T$  is the transition time calculated from:
- $$t_T = (K^2(1-v^2)) / (E(n+1)C^*(t_T)) \quad (2)$$

b) The data that meet the displacement rate requirement of  $\dot{V}_c / \dot{V} \geq 0.8$  were considered valid. The  $dV_c/dt$ ,  $\dot{V}_c$ , is the rate of creep component of deflection and  $dV/dt$ ,  $\dot{V}$ , is the rate of total deflection measured on the load line. The crack growth data,  $da/dt$  vs.  $C^*(t)$  were plotted for the data  $0.5 \leq \dot{V}_c / \dot{V} < 0.8$ , separately, and compared with the data  $\dot{V}_c / \dot{V} \geq 0.8$  for further assessment. The crack growth data obtained prior to the first 0.2mm crack extension, that may be transient creep crack growth, was identified separately.

The amount of crack deviation outside an envelope that encompasses the material between the planes that are oriented at an angle  $\theta$  [20] from the idealized plane of crack growth and that intersect the axis of loading was noted for each specimen. The amount of accumulated load-line deflection at the end of the test was also noted.

## 3. RESULTS

### 3.1 Materials

The chemical composition of the experimental materials, BM and WM, are given in Table 1. The BM values of the elements fall in the designated standard material composition range.

Table 1: Chemical composition of materials (wt. %).

Material	C	Mn	Si	P	S	Cr	Ni	Mo	V	Al	Nb	Ni+Cu
P91 BM	0.091	0.409	0.369	0.028	0.013	8.44	0.272	0.922	0.24	0.07	-	0.04
P91 WM	0.087	0.692	0.285	0.013	0.007	9.39	0.63	0.98	0.267	-	0.04	0.64

The mechanical and creep properties were determined at CCG test temperature of 600°C and depicted in Table 2. The yield strength data at test temperature show decrease in WM and particularly in HAZ-Mid. section (centre) compared with that of

BM. Therefore, the welds are undermatched in terms of yield strength values. The variation of HAZ strength values in centre and Type IV zones is also noted.

Table 2: Materials data determined in tensile and creep tests at 600°C.

Material	$R_{p0.2}$ MPa	$R_m$ MPa	E GPa	$D_1$	m	$A_1$	n
P91BM	441	463	164	0.0018	27.73	1.57E-45	18.51
P91WM	362	385	125	0.0015	23.86	5.99E-24	8.55
P91SIM. HAZ-Type IV	320	333	155	0.0016	17.38	7.16E-35	14.35
P91SIM. HAZ-Centre	293	317	139	0.0016	20.74	7.16E-35	14.09

Note: BM data were taken from EC Project HIDA (BE 1702) that used the same experimental material.

Creep deformation properties were determined at 600°C as reported in [21], and the data is given in Table 2. It is seen in Table 2 that the variation in creep properties does not follow the same sequence as the yield strength data. The creep exponent, n, is the lowest for the WM whereas HAZ-TypeIV zone has the lowest m value determined in tensile tests. The constants ( $D_1, m$ ) relate to stress-strain ( $\epsilon_p = D_1 \sigma^m$ ) and ( $A_1, n$ ) to steady-state creep ( $d\epsilon_c/dt = A_1 \sigma^n$ ) behaviour.

3.2 Metallography

The CCG specimens were sectioned after testing in the mid-thickness and prepared for optical microscopy of sectioned surfaces both in as polished and etched conditions. Figures 1a and b show micrographs of the specimen with starter notch in the HAZ-Type IV zone.

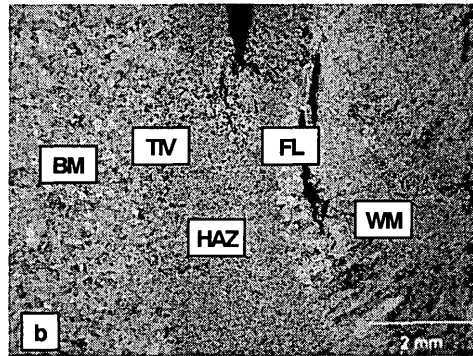
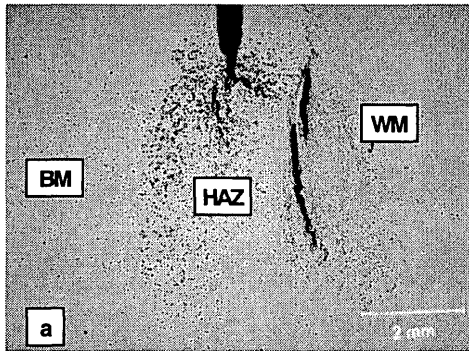


Figure 1: Optical micrograph of P91 similar weld HAZ-TIV.1. a) Polished sectioned surface showing the crack tip damage, crack initiation and growth. b) The same zone etched to reveal the crack tip microstructure.

Two points were noted in metallographic examinations: 1) damage by cavity (pore) formation at the crack tip of polished specimens, and 2) microstructure at the location of starter sharp crack (EDM Slit) and along the crack growth path in etched

specimens. Fig.1a shows extensive damage at the crack tip. A classical grain boundary creep damage is observed within a 100µm wide band across the crack growth path in WM as seen in Figure 2.

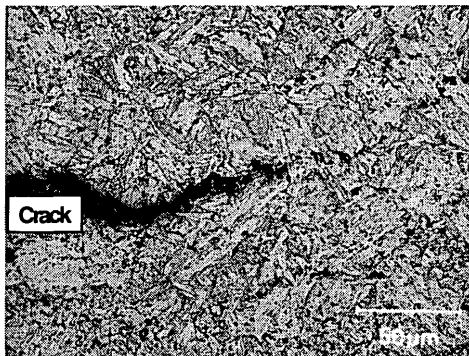


Figure 2: Optical micrograph of etched crack tip zone in WM showing the grain boundary creep damage.

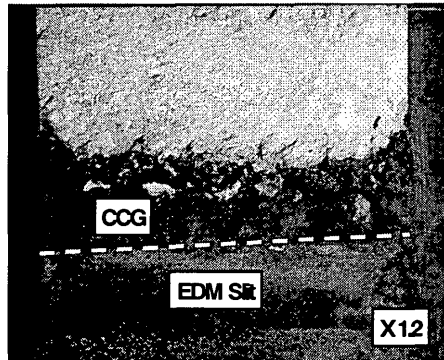


Figure 3: SEM picture of WM fracture surface of a specimen. Light unbroken ligaments are seen on oxidised fracture surface.

Fracture surface examination was carried out on selected specimens in a scanning electron microscope (SEM). Figure 3 shows the crack front irregularities and unbroken ligaments seen as unoxidized islands when broken open at room temperature. These examinations direct attention to the reliability of the DCPD method for crack growth monitoring and crack length determination.

3.3 Data Assessment and CCG Correlation

The complete experimental data was assessed and the CCG rate of specimens with starter sharp crack in WM was correlated

with crack tip parameters K and  $C^*(t)$  in Figures 4 and 5, respectively. The complete set of crack growth rate data correlate well with K, however, scatter is observed at crack growth initiation which is called tails. Note that predetermined  $K_0$  values were taken for calculating the test loads. The scatter in initiation data is reduced in  $C^*(t)$  correlation of the crack growth rate data as seen in Figure 5.

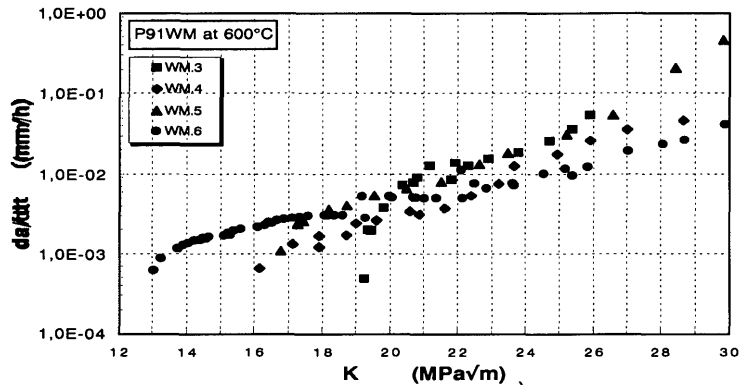


Figure 4: Creep crack growth rate as a function of K for P91WM at 600°C. Complete data set without reduction.

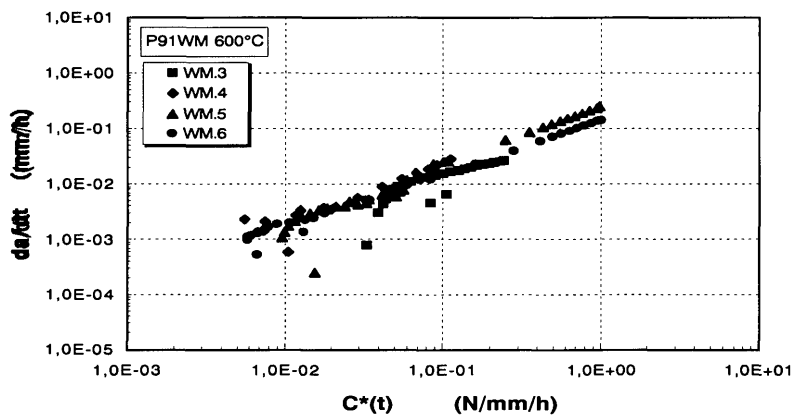


Figure 5: Creep crack growth rate as a function of  $C^*(t)$  for P91WM at 600°C. Complete data set without reduction.

The CCG data from the present work (solid symbols) is plotted together with the data from project [22] partners (Partners 1 to 3: P1-P3) in Figure 6. The data agree well with the harmonised data from partners' [21], however, the slope of the reported data with that of the linear fit line of the complete data set differs slightly, as seen in Figure 6 and Table 3. The best-fit

line data reported in [21] is summarised for the present materials in Table 3. Higher scatter in correlated HAZ crack growth rate data compared with that of WM data is seen in the good of best fit line, i.e.  $R^2$  value.

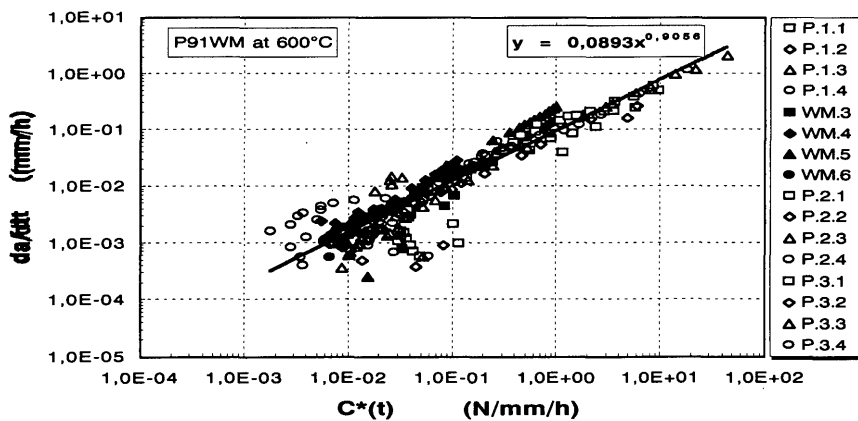


Figure 6: Creep crack growth rate as a function of  $C^*(t)$  for P91WM at 600°C. Complete project [22] data set without reduction. Partners data are indicated as P1 to P3.

Table 3: Best fit of current creep crack growth data and the complete set of project [22] partners data.  $(da/dt=DC^*(t)^q)$

Partner-Data	P91 WM	P91 HAZ
All Partners Data	D =0.089	D =0.047
	q =0.906 (R <sup>2</sup> = 0.867)	q =0.691 (R <sup>2</sup> = 0.528)
Present Reported Data	D =0.188	D =0.065
	q = 0.990 (R <sup>2</sup> = 0.892)	q = 1.024 (R <sup>2</sup> = 0.641)

The crack growth rate data of specimens with the starter crack in HAZ in centre (HAZ-MID) and TypeIV zone (HAZ-

TIV) was correlated with crack tip parameters, K and C\*(t) in Figures 7 and 8, respectively.

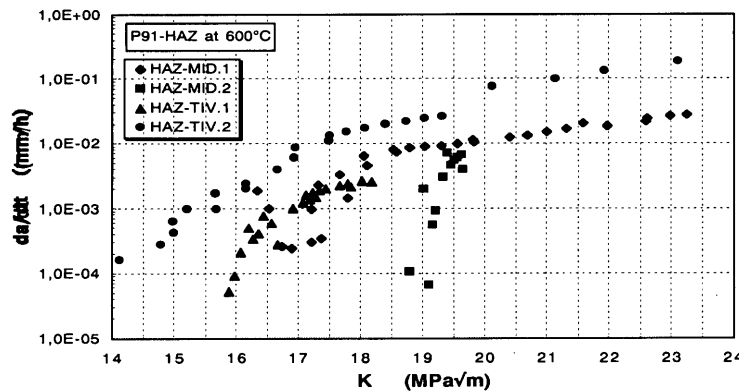


Figure 7: Creep crack growth rate as a function of K for P91HAZ at 600°C. Complete data set. The invalid test data, HAZ-MID2, is also included. Note the scatter in the crack initiation range (tails).

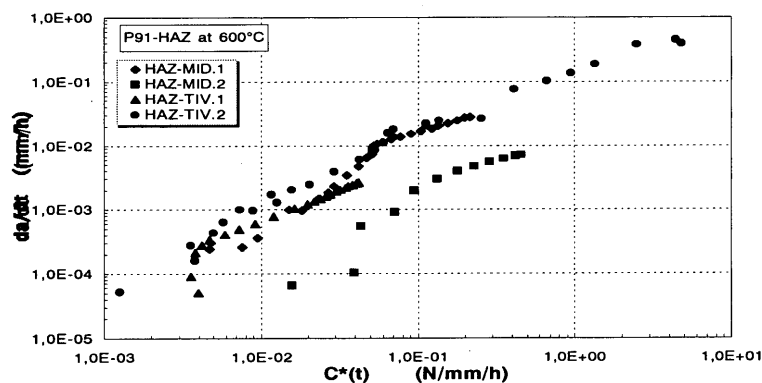


Figure 8: Creep crack growth rate as a function of C\*(t). Data from the same tests as presented in Fig.7.

The relatively brittle behaviour of HAZ together with microstructural variation along the crack path lead to higher scatter particularly in the early stages of K correlation compared with those of WM data. However, note the good correlation of crack growth rate for individual specimens.

A good correlation of CCG rate data with C\*(t) is seen in Figure 8, if the invalid test data, HAZ-MID.2, is omitted. This particular specimen data is invalid because the crack growth initiated at the fusion line, in a far location from the starter crack

tip. However, note the same slope of the invalid crack growth data as that of the valid tests'. Once the crack growth initiates regardless the starter crack position the obtained data may give the crack growth resistance of the material at the location as far as the crack tip stress state is accounted. Figure 9 depicts the present CCG rate data together with those of the project partners for specimens with initiation crack tip in HAZ. The best-fit data shown in the figure is included in Table 3 together with that of the WM.

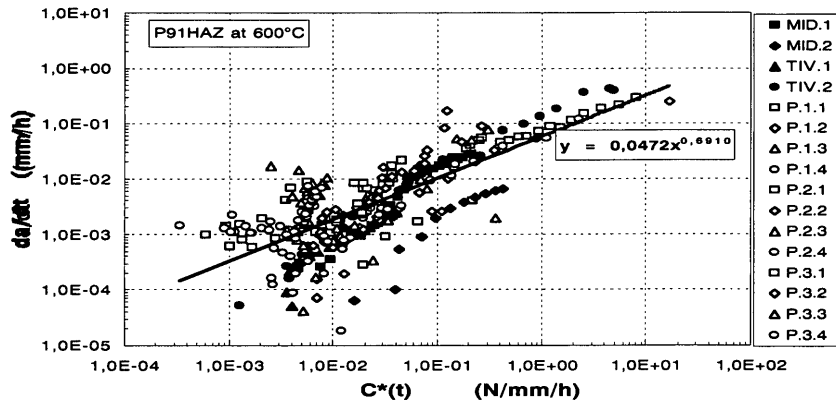


Figure 9: Creep crack growth rate as a function of  $C^*(t)$  for P91HAZ at 600°C. Complete project [22] data set without reduction.

The reduced CCG rate data for  $\Delta a > 0.2\text{mm}$  are depicted in Figures 10 and 11 for WM and HAZ, respectively. Note that the initial 0.2mm crack growth is considered as the crack growth initiation and excluded from CCG data for further processing in the ASTM E1457 (4). The data correlates well with the tails removed leading to a linear best-fit line that can subsequently be

used in structural integrity analysis. Note the invalid data HAZ-MID.2 that does not fit the valid data set whereas it may be considered as part of the initiation tails in Figure 9 due to its out of plane crack growth initiation, emphasizing the importance of data processing and analysis.

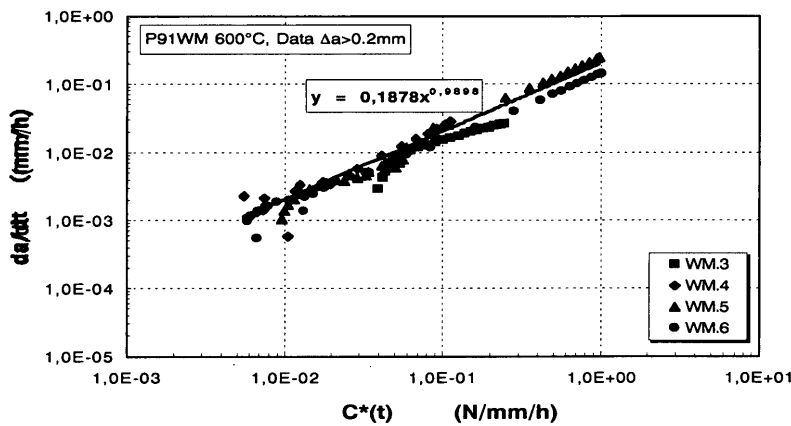


Figure 10: Creep crack growth rate as a function of  $C^*(t)$  for WM. The same data as in Fig.5, with  $\Delta a < 0.2\text{mm}$  is omitted.

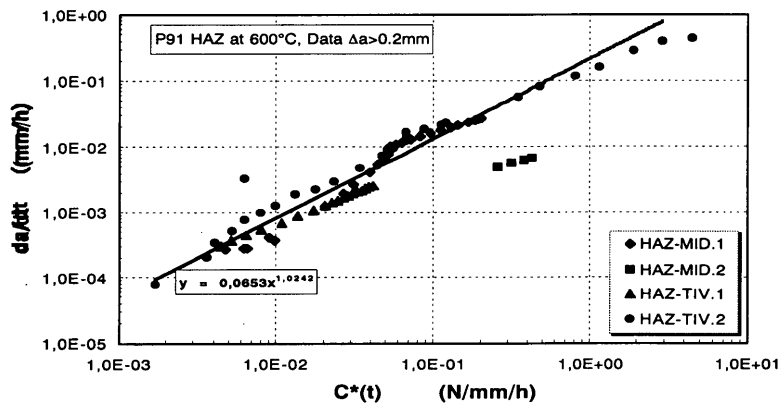


Figure 11: Creep crack growth rate as a function of  $C^*(t)$  for HAZ. The same data as in Fig.8, with  $\Delta a < 0.2\text{mm}$  is omitted.

#### 4. DISCUSSION

The increase in minimum strain rate with stress in high strength BM was higher than that of low strength WM as determined in creep tests. This result calls for consideration of the creep deformation behaviour of the material presented in terms of relative creep strain rates of BM, WM and HAZ rather than tensile strength of weldments. Therefore, creep resistant or

creep weak bond definition of welds rather than relative yield strength values in terms of overmatch-undermatch is recommended in fracture characterisation of the weldments under creep conditions.

In order to elaborate on the strength and deformation behaviour of weldments, specimens were taken for micro-hardness measurements. Surprisingly, inconsistencies in relative

hardness of weld joint constituents (i.e. BM, HAZ and WM) were noted. This may direct attention to the need for checking on the welding process. The room temperature (RT) hardness measurements indicate a relative RT strength; however, it is not indicative of creep deformation of a particular material. The creep properties must be considered in addressing the relative behaviour of individual microstructural constituents in CCG testing of weldments [21].

The metallographic information was required in assessing validity of test data for crack growth rate correlation. The crack initiation and crack growth behaviour as studied metallographically showed specimen to specimen variation, which subsequently affect the correlated crack growth data. The deformation is observed varying from extensive pore formation to classical grain boundary creep deformation as seen in Figures 1 and 2 respectively. The change in crack growth path resulted in changes in crack growth rate correlations as described below. Micrographs in Figures 1a and b are marked showing the components of welded materials as BM, WM, HAZ and TIV (TypeIV in HAZ close to BM also called by some researchers Inter Critical HAZ, ICHAZ) and FL (fusion line, also called Coarse Grained HAZ, CGHAZ). It is worth noting here that coarse or fine grained HAZ was not distinguishable in the present experimental materials. Therefore, TypeIV and FL description of zones in characterisation of weldments is emphasized.

The fracture surface examination of the crack path showed the crack front irregularities and unbroken ligaments in form of unoxidised islands. These examinations direct attention to the reliability of the DCPD method of crack growth monitoring. The calibration and correction of the predicted crack lengths with the final crack length measured on fracture surface is important. The unbroken ligaments need to be considered fractured if left behind the advancing crack front. Furthermore, the tests must be ended after 2-3mm of crack growth in order to determine a reliable crack growth data including the crack growth initiation and early crack growth.

The ASTM Standard [4] does not address testing weldments and brittle materials such as weld-HAZ. Therefore, the crack tip parameter  $K$  is included along with  $C^*(t)$  for crack growth rate correlation of weldments. The crack growth behaviour at lower growth rates is of industrial interest because a large portion of a component life may be spent in the initiation and early crack growth regime. The CCG rate data correlation with  $K$  did not reduce the scatter in initial crack growth data of complete data set. Moreover, the scatter in crack growth correlations were higher in  $K$  correlations than that in  $C^*(t)$  particularly at high crack growth rates (Fig.4). The relative brittle behaviour of HAZ together with different microstructure along the crack path led to higher scatter in  $K$  correlation compared with those of WM data. However, note the good correlation of crack growth rate for individual specimens.

The deformation is not homogeneous due to microstructural variations in weld joints. Crack growth may follow some microstructural components that are different than simulated material on which mechanical and creep data are obtained. This aspect is emphasised because the mechanical and creep data of the present WM and HAZ does not affect the CCG rate correlation if they are interchanged without considering crack tip stress and strain state and also difference in creep deformation behaviours.

Further assessment of data where initial 0.2mm crack growth data omitted, improved the correlation leading to a linear best fit with narrow scatter band. Thus presented data is used for structural integrity assessments. Although already partially addressed [21] the crack growth initiation issue still remains to be systematically studied.

The  $q$  values in  $da/dt=DC^*_{(t)}{}^q$  correlation agree well with the literature data, however, note the difference in HAZ (Table 3). The higher exponent in best fit is dictated by the long crack growth data of HAZ-TIV.2 in Figure 11. This aspect needs further investigation.

The crack growth rate correlation of WM and HAZ data may be compared in Figures 5 and 8, respectively. The crack growth rate in WM is slightly higher than the rate in HAZ, that agrees well with the reported behaviour of 1.25CrMo, 2.25 CrMo steels [1,3]. This observation related to the strain concentrations in the interface region of weldments with microstructural gradients and different creep properties. This can also explain the crack deflection and secondary cracking in weldments as seen in Figure 1. Note also that the crack deflection is traced back in the change of crack growth rates in both WM and HAZ data.

## 5. CONCLUSIONS

Reliable CCG data were obtained from tests terminated prior to final fracture in testing where the final crack length is measured on the resulting fracture surfaces after completion of the test.

Metallographic information on the crack growth path and reliable material data of local microstructure in a weld joint, (i.e. WM, HAZ Centre or HAZ Type IV), are needed in assessment of the CCG data of weldments.

The effect of material data on crack growth rate correlations with  $C^*(t)$  and  $K$  is marginal. Therefore, analytical work is needed on crack tip deformation and crack tip parameters for high temperature characterisation of weldments.

Creep resistant or creep weak bond definition of weld joints rather than relative yield strength values in terms of overmatch-undermatch is recommended in fracture characterisation of the weldments under creep conditions.

Crack growth initiates at a strained location in the weak material regardless of the starter crack position in weldment.

The CCG rate data correlates well with  $K$  and  $C^*(t)$ , provided the crack initiates at the starter crack tip and grows on the main crack plane. The scatter in  $K$  correlation is higher for HAZ than that for the WM data.

The crack growth initiation is defined at  $\Delta a=0.2\text{mm}$ . However, early crack growth data with  $\Delta a<0.2\text{mm}$  should not be discarded due to its relevance to component behaviour in service. Crack growth initiation needs to be systematically studied for structural assessment of welded components at high temperature.

## 6. ACKNOWLEDGEMENTS

The author would like to thank B.Petrovski of T.U.Darmstadt for scientific discussions and support, and the European Commission (EC) for their financial contribution and the partners for their contribution in the EC Project SOTA: - 'Development of Creep Crack Growth Testing and Data Analysis Procedures for Welds': ENEL (IT), ERA Technology (UK), Iberdrola (ES), JRC-Petten (NL), EDP/ISQ (PT), SAQ Kontroll/SIMR (SE).

## 7. REFERENCES

- [1] Holdsworth, S., Proc. Int. Conf. On Integrity of High Temperature Welds, Org. by IOM Comm. and I Mech. E, Professional Eng. Publ. Ltd. U.K. (1998), pp.155-166.
- [2] Parker, J.D., Proc. Int. Conf. On Integrity of High Temperature Welds, Org. by IOM Comm. and I Mech. E, Professional Eng. Publ. Ltd. U.K. (1998), pp.143-152.
- [3] Saxena, A., Nonlinear Fracture Mechanics for Engineers, CRC Press LLC, Boca Raton FL, USA, (1988), pp.384-389.
- [4] ASTM E1457-98, Standard Test Method for Measurement of Creep Crack Growth Rates in Metals, ASTM 03.01, ASTM, Philadelphia, PA 19103, USA, (1997).

- [5] Saxena, A and Liaw, P.K., "Remaining Life Assessment of Boiler Pressure Parts-Crack Growth Studies", EPRI CS 4688, Electric Power Research Institute, Palo Alto, CA, (1986).
- [6] Dogan, B., Saxena, A. and Schwalbe, K.-H., *Materials at High Temperatures*, Vol.10, No.2, May (1992), pp.138-143.
- [7] Dogan, B. and Petrovski, B., *Int. Conf. "Integrity of High Temperature Welds"* Forte Posthouse, Nottingham, U.K., 3-4. 11.1998.
- [8] Riedel, H. and Detampel, V., *International Journal of Fracture*, Vol.36, (1988), pp.275-289.
- [9] Hawk, D.E. and Bassani, J.L., *Journal of the Mechanics and Physics of Solids*, Vol.34, No.3, (1986), pp.191-212.
- [10] *Engineering Fracture Mechanics, Special Issue on Crack Growth in Creep-Brittle Materials*, Eds. Saxena A. and Yokobori T., Vol.62, No.1, (1999).
- [11] Ainsworth, R.A., The initiation of creep crack growth, *Int J. Solids Structures*, Vol.18, No.10, (1982), pp.873-881.
- [12] Neate, G.J., Creep crack growth behaviour in 0.5CrMoV steel at 838K, *Mat Sci. Eng.*, Vol.82, (1986), Part I: Behaviour at a constant load, p.59-76; Part II: Behaviour under displacement controlled loading, pp.77-84.
- [13] Saxena, A., Creep crack growth under non steady-state conditions, *ASTM STP905*, (1986), pp.185-201.
- [14] Riedel, H., *Fracture at High Temperatures*, MRE-Springer Verlag, (1987).
- [15] Holdsworth, S.R., Initiation and early growth of creep cracks from pre-existing defects, *Materials at High Temperatures*, Vol.10, No.2, (1992), pp.127-137.
- [16] *Stahl-Eisen-Werkstoffblatt 088 1. Ausgabe.*
- [17] *AWS Welding Handbook*, Vol.1, p.86.
- [18] Saxena, A., Dogan, B. and Schwalbe, K.-H., Evaluation of the Relationship Between  $C^*$ ,  $\delta_5$  and  $\delta_t$  during Creep Crack Growth, *ASTM STP 1207*, ASTM, Philadelphia, (1994), pp.510-526.
- [19] Dogan, B., Martens, H., Blom, K.-H., and Schwalbe, K.-H., *Conf. Proc. LASER 5, IITT Int. Conf.*, 10-11 April 1989, London, (1989), pp.188-194.
- [20] *ASTM E647-95, Standard Test Method for Measurement of Fatigue Crack Growth Rates*, ASTM, Philadelphia, PA 19103, USA.
- [21] Dogan, B. and Petrovski, B., *Int. Conf. HIDA-2, MPA-Stuttgart*, 04-06.10.2000, Stuttgart, Germany, to be published in a special issue of *Int. J. of Pressure Vessels and Piping*, (2001).
- [22] EC Project SOTA: SMT 2070. Development of Creep Crack Growth testing and Data Analysis Procedures for Welds.